Volume 1
Number 8
November 2023
Pages 1899–2108

RSC Sustainability

rsc.li/rscsus

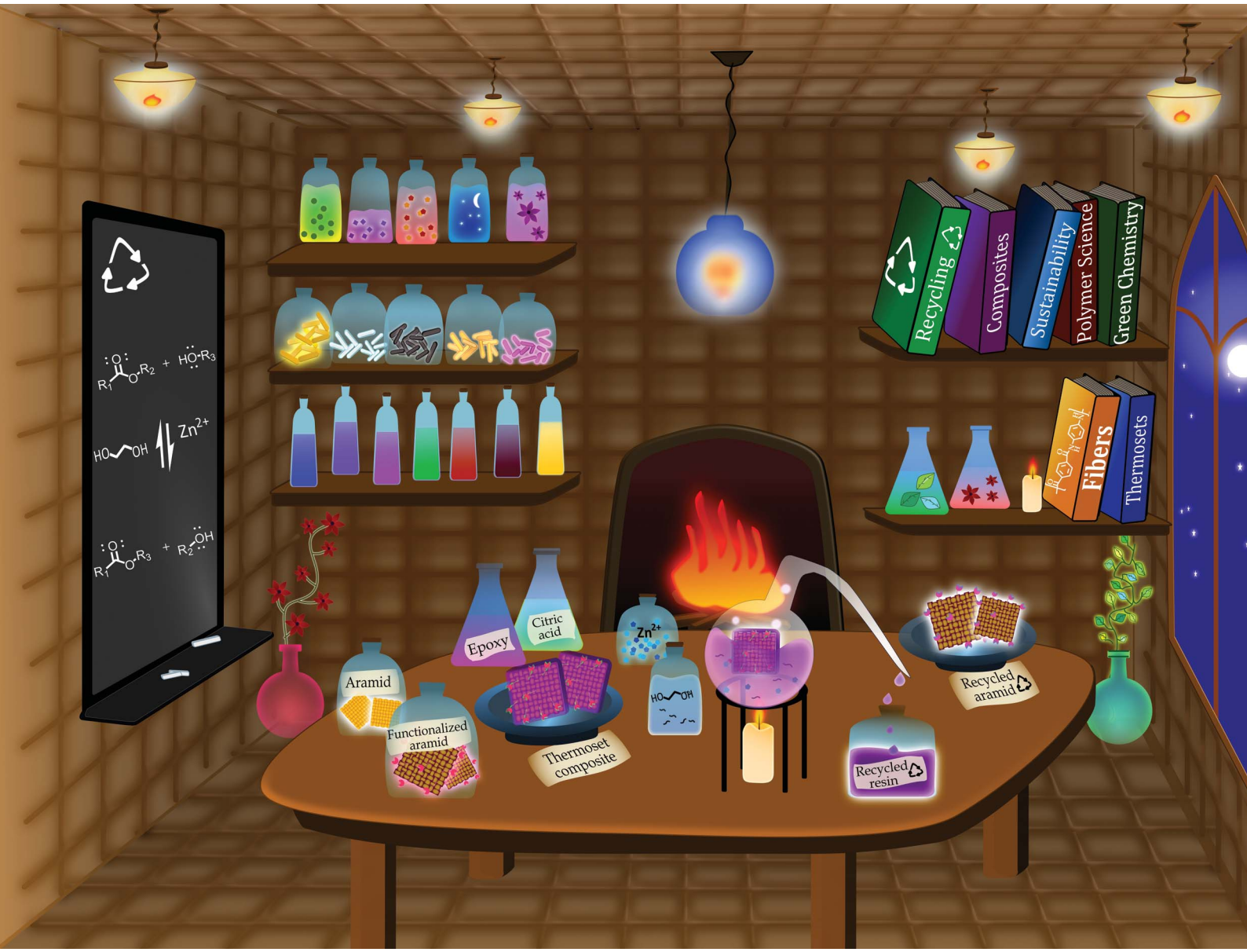

ISSN 2753-8125

ROYAL SOCIETY OF CHEMISTRY

PAPER
Minna Hakkarainen *et al.*
Surface modification of aramid fiber meshes – the key to chemically recyclable epoxy composites

RSC Sustainability

ROYAL SOCIETY OF CHEMISTRY

PAPER

View Article Online
View Journal | View Issue

Cite this: *RSC Sustainability*, 2023, **1**, 1967

Surface modification of aramid fiber meshes – the key to chemically recyclable epoxy composites†

Karla Garfias, [ab] Inger Odnevall, [c] Karin Odelius [ab] and Minna Hakkarainen *[ab]

The higher chemical sensitivity of aramid fibers, compared to carbon or glass fibers, adds to the challenge of designing recyclable aramid fiber reinforced polymer composites. Our study sheds some light on this endeavor through a surface functionalization approach. Twaron® aramid fibers were surface modified by self-polymerization of dopamine followed by the condensation of a silane coupling agent, bearing an epoxy group (PDA-Si). Thanks to the mild modification process, the fibers retained their thermal and mechanical properties. At the same time, the functionalization enhanced the adhesion strength between the meshes and a partially bio-based epoxy thermoset, which was demonstrated by a peeling adhesion test and lap-shear bonding test. Chemical recycling of the epoxy thermoset and epoxy composites reinforced with PDA-Si aramid meshes was achieved by mild solvolysis in ethylene glycol. The recycled thermoset was rich in hydroxyl groups, which promoted the adhesion with PDA-Si meshes. Furthermore, high-quality PDA-Si aramid meshes were recovered after the chemical recycling. The recovered meshes showed 82% removal of the thermoset matrix and the retention of the surface functionalization as suggested by thermogravimetric and spectroscopic analyses, respectively. This enabled 78% recovery of the initial interface strength between the recycled PDA-Si meshes and virgin thermoset matrix. This unveils the role of surface functionalization not only as a performance enhancer but also as a useful aid in the development of circular FRPCs.

Received 28th July 2023
Accepted 19th September 2023

DOI: 10.1039/d3su00258f

rsc.li/rscsus

Sustainability spotlight

The demand for fiber reinforced polymer composites (FRPCs) keeps increasing due to the beneficial balance between light weight and high performance. However, the strategies to recycle these materials after use lack behind. Here we developed a fiber surface functionalization technique that serves as a bridge between both tasks; it promotes a strong interface between the fibre and matrix to achieve durable and high-performance products and at the same time, it facilitates the chemical recyclability after use. The work thereby aligns with UN Sustainable Development Goals, especially Goal 9 "Industry, innovation and infrastructure", through the design of quality and resilient products and encompasses Goal 12 "Responsible consumption and production", by preventing and reducing waste through an improved recycling approach, which promotes circularity.

1 Introduction

Modern society, as we know it, cannot be conceived without plastics. However, the negative impact that they can impose on the environment is undeniable and more sustainable alternatives are needed to maintain our quality of life, without further endangering our environment. An increase in the durability of the material and design for circularity are crucial.[1] In light of this, the urge for sustainable solutions for fiber reinforced polymer composites (FRPCs) is pressing.

FRPCs are composed of high-performance fibers such as carbon fibers, glass fibers or aramid fibers which can be embedded in thermoplastic or thermoset polymer matrixes. When it comes to highly demanding applications, thermoset polymer matrixes such as epoxy resins or elastomers are undoubtedly an attractive option, because of their unparallel mechanical strength and thermal and chemical stability. FRPCs have long benefited from different fiber functionalization techniques such as surface etching,[2,3] RFL coating,[4,5] plasma treatments[4,6–8] and adhesion activated systems[5,9] to enhance the performance of the composite products.

The self-polymerization of dopamine has been reported as a new functionalization methodology, which has been applied on carbon fibers,[10–12] glass fibers[12] and aramids.[13–16] Additionally, the active functional groups of polydopamine have been

[a]*Department of Fiber and Polymer Technology, KTH Royal Institute of Technology, Teknikringen 56-58, 100 44 Stockholm, Sweden. E-mail: minna@kth.se*

[b]*DPI, P.O. Box 902, 5600 AX Eindhoven, the Netherlands*

[c]*Division of Surface and Corrosion Science, KTH Royal Institute of Technology, 100 44 Stockholm, Sweden*

† Electronic supplementary information (ESI) available. See DOI: https://doi.org/10.1039/d3su00258f

used for further functionalization steps (Fig. S1†).[17] For example, the hydroxyl groups from the catechol structure can participate in the condensation with silane coupling agents bearing amine moieties[18] and epoxy groups.[16] This methodology has proved to be mild and has resulted in an increase in the interface strength between the fibers and commercial epoxy resins,[19–22] which can contribute to materials with increased performance and durability.

Thermoset FRPCs have a highly crosslinked structure containing strong covalent bonds that cannot be melted or dissolved making it difficult to design recycling strategies and to recover other than low value products.[23,24] Current strategies consist of incineration and shredding; however, these methodologies are not sustainable enough as they unavoidably lead to downgrading the value of the material.[1] In contrast, certain chemical recycling methods can offer the possibility to recover high-value fibers. This has been implemented with the help of super/sub-critical fluids, molten salts, electrochemical processes or matrix digestion in strong oxidant or acidic environments.[25,26] Yet, these techniques typically lead to degradation of the thermoset matrix preventing its reuse.

Chemical recycling through mild solvolysis has proven to be a suitable alternative to recover both components. It has been shown that the incorporation of labile cross-linking points into the thermoset matrix enables the application of chemical recycling under relatively mild conditions. For example, ester bonds in epoxy thermoset matrixes have been successfully reversed through acidic and basic hydrolysis,[27–31] aminolysis[25] and alcoholysis through transesterification exchange reactions.[29,31–34] This concept has been applied mainly to carbon fiber[23,24,32,35–37] and glass fiber[38] epoxy composites. Presumably due to the higher chemical sensitivity of aramid, the reports on chemical recycling of aramid fiber composites through such methods are scarce. A pioneering study proved that it is possible to recover aramid fibers from a cross-linked network based on amide bonds.[39] The composite was successfully recycled by triggering Diels–Alder reactions.

High-performance composites usually require treatment of reinforcing fibers with sizing or with specific surface functionalization in order to enhance the adhesion strength for the required properties. However, the role of surface functionalization in the chemical recycling of FRPCs has been largely overlooked. In a recent example, formic acid digestion of a carbon fiber reinforced epoxy composite led to the loss of the fiber sizing, which was then related to a slight loss of properties.[40] Addressing the role of the fiber functionalization in the development of future chemical recycling methodologies is therefore of high importance.

Our work dives into two of the main sustainability challenges encountered for aramid reinforced epoxy composites, namely an increase in the lifespan of the material and better recycling strategies. We believe that fiber surface functionalization can be a key to avoid early composite failure such as debonding and delamination and at the same time it can be beneficial in the chemical recycling process of aramid composites. We envision that proper fiber functionalization can improve the quality of the recovered fibers and promote circularity. Therefore, we surface functionalized Twaron® aramid fibers with polydopamine, followed by the condensation of a silane coupling agent bearing an epoxy group. Thereafter, the interface strength between the obtained fibers and an epoxy thermoset cured with citric acid (TVx) was assessed. The formation of an ester based network enabled chemical recyclability through hydrolysis and mild solvolysis by transesterification exchange reactions.[29,41,42] The recovered thermoset polymer matrix (TRx) and functionalized aramid meshes (r-PDA-Si) were spectroscopically, microscopically and thermally characterized and the possibility to reuse the recovered components in similar applications was further evaluated.

2 Experimental

2.1 Materials

Unmodified (UA) Twaron® *para*-aramid fibers of 12 μm diameter were kindly supplied by Teijin Aramid B.V. in two different forms: aramid yarns of 1680 decitex (dtex) and aramid meshes with dimensions of 50 cm length, 15 cm width and a thickness of around 0.67 mm. The meshes were treated with a spin finish based on a fatty acid ester, required to facilitate the weaving process, washed with water and laser-cut at Teijin before delivery. The yarns were specially produced without spin finish for this project.

Dopamine hydrochloride (≥99.8%), tris(hydroxymethyl) amino methane (TRIS) (≥99.8%), and the silane coupling agent (3-glycidyloxypropyl)trimethoxysilane (98%) were all purchased from Sigma-Aldrich, Sweden. Ethanol (technical grade 99.98%) was purchased from VWR, Sweden and used in a water mixture to wash the fibers. Thermosets and composites were prepared with the epoxy resin trimethylolpropane triglycidyl ether (technical grade with an epoxy equivalent of 140 g per equivalent) and citric acid (≥99.5%) as the curing agent, which were purchased from Sigma-Aldrich, Sweden. The reagents to evaluate the chemical recycling consisted of HCl (37% vol) and ethylene glycol (≥99.8%), purchased from Sigma-Aldrich, Sweden; zinc acetate dihydrate (≥99.99%) and NaOH (≥97%) purchased from VWR, Sweden. All chemicals and solvents were used without further purification.

2.2 Aramid functionalization and Soxhlet extraction

Surface functionalization was performed on aramid yarns and aramid meshes. Single filaments from the yarns were used to properly evaluate the fiber topography and the impact of the surface functionalization on the mechanical and thermal properties. The meshes were spectroscopically characterized and used for composite preparation, adhesion strength characterization and chemical recycling.

Before functionalization, the unmodified aramid yarns (UA) were rinsed with a cleaning solution of a 50/50 v/v mixture of water and ethanol to eliminate impurities. The fiber meshes were cut into squared pieces of 10 cm × 10 cm and submerged in this cleaning solution at 60 °C for 2 h to clean any possible remnants of the finish.

The first functionalization step consisted of the self-polymerization of dopamine and was adapted from previously reported methods.[16,17] In short, unmodified aramid (UA) yarns or meshes were immersed in 150 mL of a dopamine hydrochloride solution with a concentration of 2 g L^{-1} and a pH of 8.5 stabilized with TRIS buffer. The yarns/meshes were left in the solution for 24 h at room temperature. Thereafter the functionalized material was washed several times with water until neutral pH was achieved and the cleaning water remained colorless. In the second step, polydopamine (PDA) coated yarns/meshes were immersed in 150 mL of an aqueous solution of the silane coupling agent at a concentration of 2 wt%. (i) The yarns/meshes (PDA-Si) were left in the solution for 6 h at 60 °C, rinsed with water/ethanol cleaning solution and dried under vacuum at room temperature for at least 72 h. To evaluate the stability of the functionalized layers, an extraction procedure was conducted. For that aim, one meter of functionalized yarns was subjected to Soxhlet extraction in ethanol for 24 h.‡

2.3 Thermoset and composite preparation

The virgin thermoset (TVx) and composites with virgin unmodified and functionalized aramid meshes were prepared by dissolving 4.47 g of citric acid in 3 mL of distilled water at 60 °C. Thereafter, 10 g of trimethylolpropane triglycidyl ether was added and a blurry mixture was obtained. The reaction mixture was kept under stirring at 60 °C until a translucid viscous mixture was formed. Thereafter, the mixture was poured into a squared aluminum mold of 8 cm × 8 cm, which was previously covered with a Teflon film of 0.1 mm thickness to facilitate demolding. Composite pre-pregs were prepared with meshes of virgin unmodified aramid (v-UA), polydopamine coated aramid (v-PDA) and polydopamine-silane functionalized (v-PDA Si), and the meshes were submerged in a mold with dimensions of 5 cm × 10 cm containing 6 g of the described resin mixture. The virgin thermoset (TVx) and virgin composites (v-UA, v-PDA and v-PDA-Si) were thereafter pre-cured in an oven at 80 °C for 2 h followed by 24 h at 110 °C. As a subsequent step, two pieces of the pre-cured material were placed on top of each other in a mold with dimensions of 7 cm × 6 cm x 1.3 cm as shown in Fig. S2g† and hot pressed at 180 °C and 250 kN for 1 h in a TP 400 instrument from Fontune Presses. This led to the obtention of bi-layered composites for further characterization and evaluation.

2.4 Chemical recycling

Three chemical recycling methods were evaluated. Acid hydrolysis was assessed by submerging 10 g of cured virgin thermoset (TVx) in 100 mL of a solution of 1 M HCl. The solution was left under mild stirring at 60 °C for 24 h. Basic hydrolysis was applied on the cured TVx and the cured PDA-Si composite by submerging 10 g of TVx or PDA-$Si_{composite}$ in 100 mL of a 1 M NaOH solution for 30 min at 80 °C. A mild solvolysis to trigger transesterification exchange reactions was evaluated on the TVx thermoset and $UA_{composite}$, $PDA_{composite}$ and PDA-$Si_{composite}$. For that aim, a 10 g piece of TVx or the respective composite was introduced into 100 mL of ethylene glycol containing 100 mg of zinc acetate. The reaction mixture was left overnight under mild agitation at 180 °C.

The specimens discussed in the subsequent sections are abbreviated as follows:

Virgin meshes with virgin thermosets:
v-UA_TVx, v-PDA_TVx, and v-PDA-Si_TVx
Virgin meshes with recycled thermosets:
v-UA_TRx, v-PDA_TRx, and v-PDA-Si_TRx
Recycled meshes with virgin thermosets:
r-UA_TVx, r-PDA_TVx, and r-PDA-Si_TVx

3 Results and discussion

Surface functionalization of aramid meshes was developed to facilitate chemical recyclability and to simultaneously improve the interfacial strength between the aramid mesh and epoxy thermoset matrix before and after chemical recycling.

3.1 Fiber functionalization

To functionalize aramid fibers, the aramid surface was first activated by the self-polymerization of dopamine. This resulted in a clear change in color from yellow to dark brown (Fig. 1a). As a next step, catechol groups in polydopamine (PDA) were utilized to enable the condensation reaction of a silane coupling agent bearing an epoxy group[16] (PDA-Si) with no further change in color during this reaction step.

3.2 Spectroscopic characterization of functionalized fibers

The chemical composition of the functionalized layers was ascertained by ATR-FTIR, SEM-EDS and XPS. The characteristic bands associated with the structure of *p*-phenylene terephthalamide (3310 cm^{-1} N–H stretching; 1635 cm^{-1} C═O amide I stretching; 1538 cm^{-1} and 1515 cm^{-1} N–H bending vibrations) are clearly observed in the acquired spectra of virgin UA (Fig. 2a). The polydopamine coating (v-PDA) caused a broader band around 3305 cm^{-1} and a shoulder around 1216 cm^{-1} associated with the O–H stretching vibrations of the catechol units in PDA. The clear shoulder observed at 1612 cm^{-1} can be associated with the conjugated carbonyl groups from the quinone structure. The bands associated with N–H bending vibrations presented a shift towards lower wavenumbers, and additionally a broad shoulder at 1473 cm^{-1} and 1403 cm^{-1} was observed and assigned to the amine and imine groups in PDA. In agreement with previous studies,[16] the epoxy functionalization (v-PDA-Si) resulted in the appearance of new bands associated with the structure of the silane coupling agent. In short, the C–H stretching vibrations from the aliphatic structure were observed at 2923 cm^{-1} and 2871 cm^{-1}. Additionally, the bands at 1201 cm^{-1} and 1059 cm^{-1} can be assigned to Si–O and Si–O–C stretching vibrations, respectively. Furthermore, the presence of the epoxy functionality was suggested by the shoulder at

‡ Detailed description of experimental methods (SEM, SEM-EDS, AFM, XPS, FTIR, TGA, DSC, NMR, SEC, lap shear tests, single fiber tensile tests, and peeling tests) and further details concerning sample preparation.

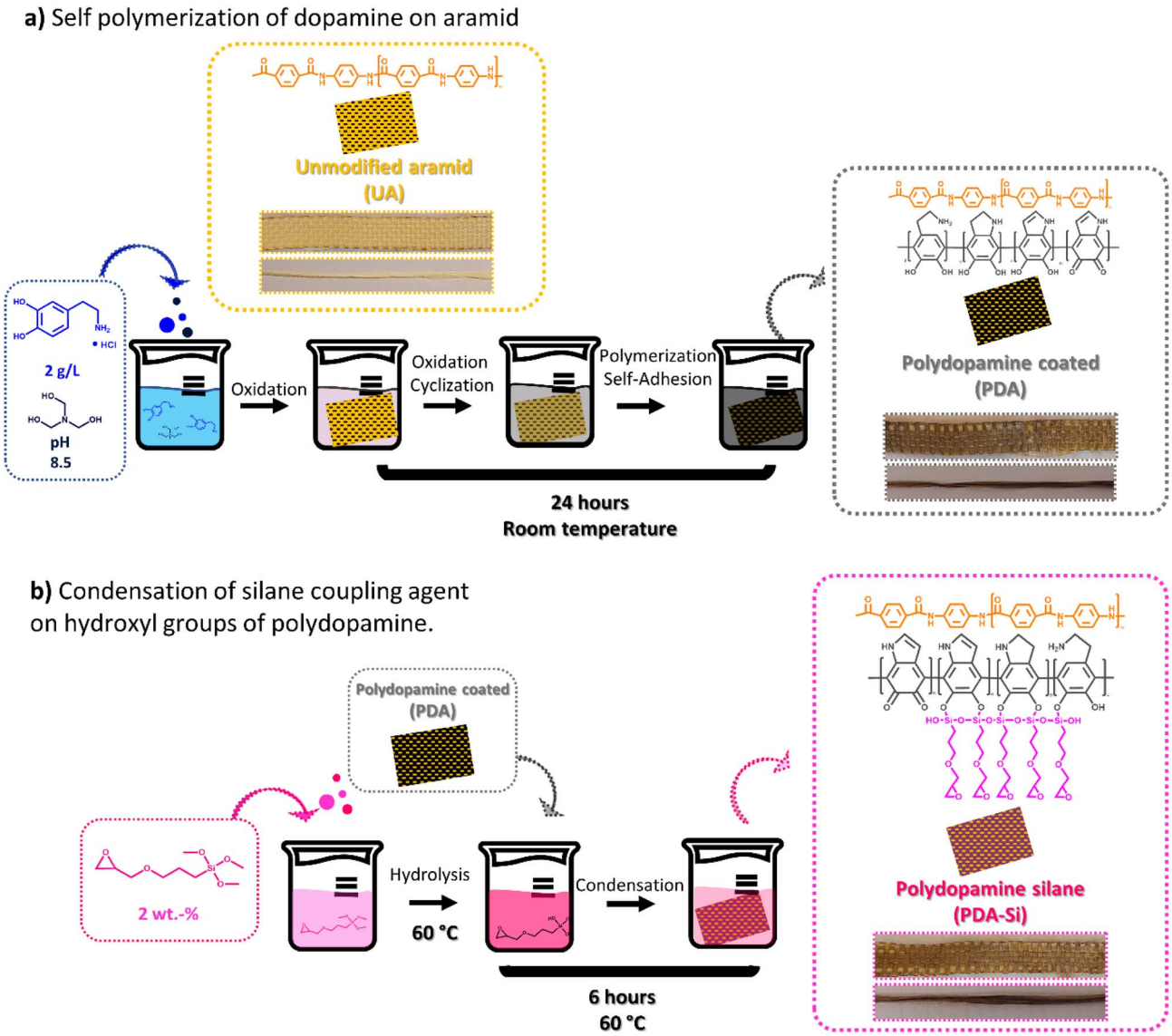

Fig. 1 The experimental setup followed to functionalize unmodified aramid fibers and meshes in two steps. (a) Self polymerization of dopamine. (b) Condensation of a silane coupling agent.

1251 cm^{-1} corresponding to the C–O stretches and at 911 cm^{-1} assigned to the epoxy ring vibrations.

The presence of the silanized layer was further ascertained by SEM-EDS and XPS, which revealed a 5-fold increase in the concentration of silicon atoms on the surface of v-PDA-Si meshes when compared to v-UA and v-PDA (Fig. 2b). The slight presence of silicon detected on v-UA and v-PDA can be explained by contamination from high-vacuum silicon grease.

The atomic percentages of detected elements were quantified using both techniques and compared with the theoretical values, Table 1. It should be emphasized that XPS provides information of the composition at the outermost surface (5 10 nm), whereas EDS reflects the composition with μm-depth resolution. The analysis of the atomic percentage of unmodified aramid (v-UA) showed a higher amount of oxygen and a lower amount of nitrogen than expected, which can be explained by the presence of some remnants of the standard finish and the possible contamination from adventitious carbon species from ambient air. The atomic ratios of the aramid fibers treated with polydopamine (v-PDA) are in close agreement with the expected values calculated from the reported structure of polydopamine, and the slightly higher oxygen content can be explained by the possible formation of carboxylic structures as reported in other studies (Fig. S1b†).[43–45]

The theoretical atomic percentage of v-PDA-Si was calculated considering that the quinone moiety of polydopamine cannot condensate with the silanol units of the coupling agent. Therefore, the presence of polydopamine is expected to have a slight influence on the detected atomic percentage. In line with the above, v-PDA-Si meshes exhibited a considerable drop in the concentration of nitrogen and a significant increase in the atomic percentage of oxygen. This observation is the result

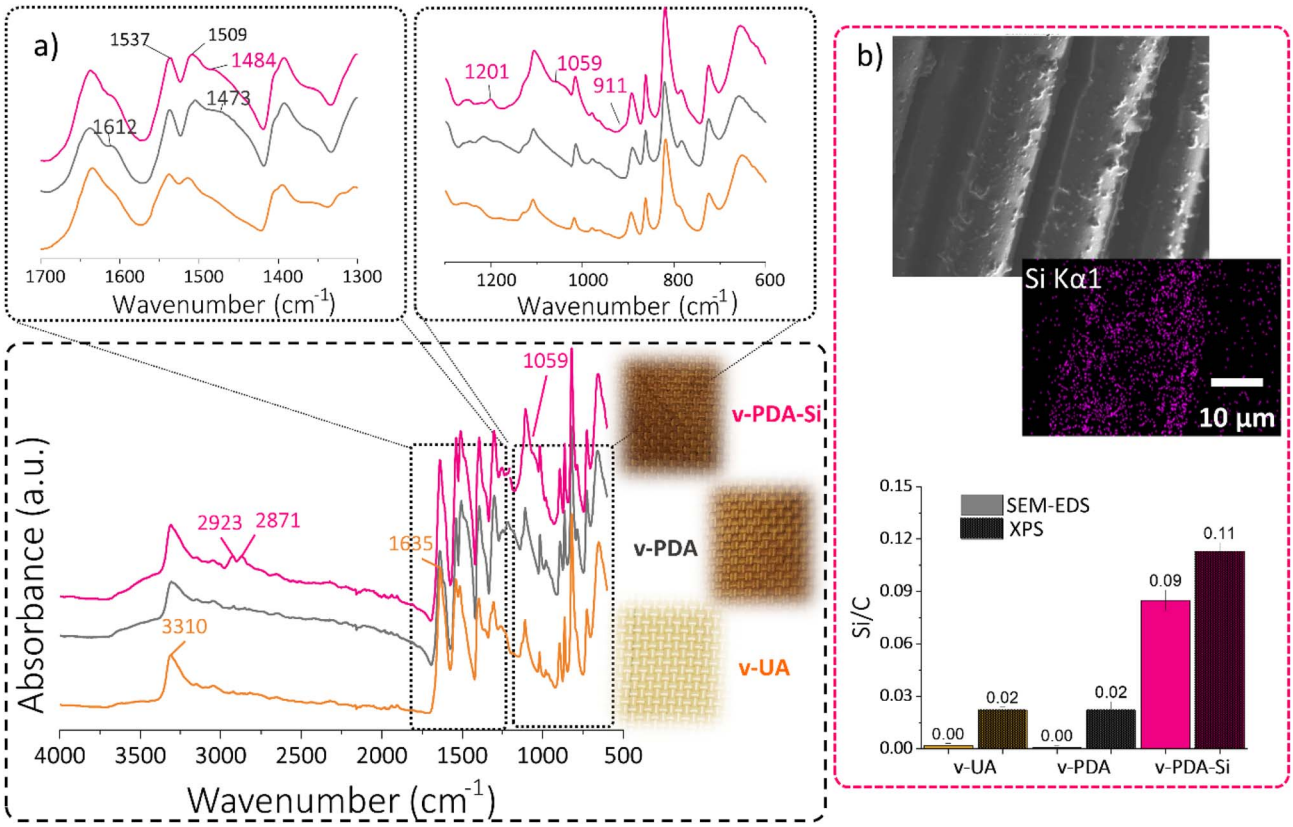

Fig. 2 Spectroscopic characterization of virgin aramid meshes of unmodified aramid (v-UA), polydopamine coated (PDA) and polydopamine silane functionalized (PDA-Si). (a) Acquired ATR FTIR spectra. (b) SEM-EDS mapping image of PDA-Si meshes and Si/C ratios determined by means of EDS and XPS measurements on the virgin meshes.

Table 1 Atomic percentages of elements detected and quantified by means of XPS (outermost surface composition – top 5–10 nm) and SEM-EDS (bulk composition – sub-µm information), compared against theoretical values[a]

	C	O	N	Si	Cl	Ca
v-UA$_{XPS}$	75.4	16.9	6.3	1.6	—	—
v-UA$_{EDS}$	75.4	13.1	11.3	0.2		
v-UA$_{Theor}$	77.8	11.1	11.1	—	—	—
v-PDA$_{XPS}$	71.7	19.2	7.1	1.6	0.4	—
v-PDA$_{EDS}$	75.2	16.2	8.5	0.1	—	—
v-PDA$_{Theor}$	72.7	18.2	9.1	—	—	—
v-PDA-Si$_{XPS}$	64.2	27.8	0.5	7.2	—	0.3
v-PDA-Si$_{EDS}$	64.6	25.5	4.3	5.5	—	—
v-PDA-Si$_{Theor}$	54.3	35.7	1.4	8.6	—	—

[a] XPS and EDS refer to experimental values, Theor. refers to theoretical atomic percentage values. Complete analysis of the atomic percentages and deconvoluted curves of UA and PDA meshes is presented in the ESI.

of the chemical structure of the coupling agent, which is rich in oxygen and silicon, but contains no nitrogen. Therefore, some of the nitrogen signals from the underneath layers of PDA and aramid are covered. This tendency is also reflected in the higher O/C and Si/C atomic ratios reported in Table S1.†

The analysis of the deconvoluted curves from the C 1s spectra of v-UA (Fig. 3a) conforms with the expected structure of the *p*-phenylene amide by the presence of characteristic signals described in previous studies[5,8,9,16,46,47] (O 1s, N 1s and Si 2p curves are displayed in Fig. S3†). The analysis of the deconvoluted curves of the C 1s spectra (Fig. 3b) and N 1s and O 1s in Fig. S4† further suggests that the structure of the coating in v-PDA contains carboxylic units and $^{+}NH_3$ species. On the other hand, the analysis of v-PDA-Si spectra indicates the presence of a silanized layer. The C 1s spectra (Fig. 3c) showed an increased intensity in the C–O and C–O–C signals at 286.3 eV and 286.8 eV, respectively, which can be ascribed to the functional groups in the structure of the silane coupling agent and suggests the presence of epoxy groups. Additionally, the O 1s and Si 2p spectra in Fig. 3e and f, respectively, showed the presence of signals at 533.5 eV and 103.1 eV which can be associated with the formation of O–Si–O bonds characteristic of the condensation of the silane coupling agent.

3.3 Fiber topography

Fiber topography is a relevant surface feature, which is not only intrinsic to the surface functionalization, but it can also have an impact on the adhesion properties. The morphology on the fiber surface was microscopically characterized after each functionalization step by means of SEM and AFM. The SEM images depicted in Fig. 4 clearly show that the neat surface of unmodified aramid changed dramatically to a rough structure

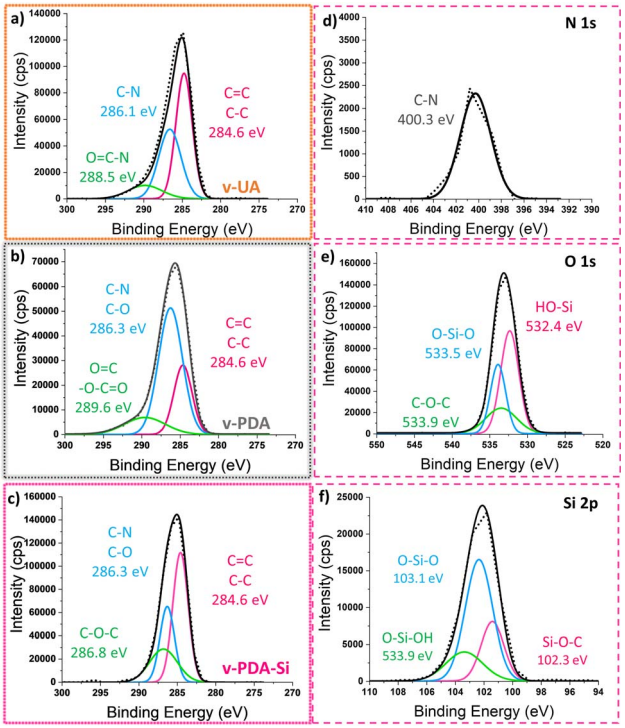

Fig. 3 XPS analysis. C 1s high resolution spectra of (a) virgin unmodified aramid (v-UA), (b) virgin polydopamine coated aramid (v-PDA), and (c) virgin polydopamine-silane functionalized aramid (v-PDA-Si). (d) N 1s, (e) O 1s and (f) Si 2p high resolution spectra of v-PDA-Si. The images include the analysis of deconvoluted curves and functional groups assigned to the fitted peaks. Dashed black lines correspond to the experimental curve. Solid black lines correspond to the fitted envelop.

due to the presence of polydopamine particles of varying sizes ranging from 30 nm to 2 μm. The micrometer sized PDA particles measured on the surface of the fibers are within the values reported previously in overnight setups with TRIS buffer solutions.[45]

After silanization, the SEM images of PDA-Si fibers revealed a subsequent change in the morphology and size of the surface features with diameters in the range of 100 nm to 2.5 μm.

A deeper insight into the change in topography was achieved by AFM. The morphology of unmodified aramid depicts the presence of small irregularities on the surface, mainly consisting of dispersed holes with a depth of less than 2 nm. This feature was previously observed in the core of Twaron fibers and was explained by the solvent removal procedure, which potentially can lead to shrinkage favoring the formation of voids.[48] A clearly different pattern was observed for the aramid fibers with dopamine coating, where dispersed aggregates with a maximum and average height of 89 nm and 37 nm respectively were observed. The obtained results agree with the reported values under similar coating conditions that typically lead to rough agglomerates with thicknesses ranging from a few nanometers to 100 nm.[49] The subsequent silanization procedure led to a further increase in the maximum height (109 nm), average height (42 nm) and roughness values (15.7 nm), which agrees with the further changes in the fiber morphology observed by SEM.

3.4 Thermogravimetric analysis and single fiber tensile test

Surface functionalization can deteriorate the thermal resistance and tensile strength of aramid fibers. However, the results from TGA and single fiber tensile tests confirmed that the mild functionalization conditions to obtain PDA-Si fibers did not lead to a decline in those essential properties (Fig. 4f, g, Tables S2 and S3†).

3.5 Thermoset preparation

Epoxy thermosets with ester based cross-linking points were achieved by the curing reaction between an aliphatic tri-epoxy resin and an aqueous solution of citric acid (Fig. 6a). The curing reaction between epoxy groups and carboxylic acids tends to be slow and can lead to a number of side reactions. However, the dissociation of citric acid in water can lead to acidic protons, which can potentially catalyze the formation of ester bonds in an aqueous solution without the need for an external catalyst and toxic solvents (Fig. S5†).[30,50–53] The curing reaction was evaluated by ATR-FTIR. The acquired spectra of the cured TVx (Fig. S6†) depicted the disappearance of the bands at 908 cm^{-1} and 3055 cm^{-1} associated with the vibrations of the epoxide ring. Additionally, the two bands observed in the carbonyl region at 1708 cm^{-1} and 1631 cm^{-1} corresponding to the C=O stretching of carboxylates (Fig. S6†) presented a shift to 1731 cm^{-1} and 1643 cm^{-1}, which together with the new band at 1181 cm^{-1}, corresponding to the O C=O stretching vibrations, suggest the formation of ester based crosslinking points. The presence of β hydroxyl groups as a result of the ring opening reaction was proposed by the appearance of a broad band around 3418 cm^{-1} associated with the O–H stretching vibrations of tertiary alcohols.[54] Furthermore, the curing behavior of the thermoset was followed by differential scanning calorimetry. The thermograms in Fig. S7a† depict an exothermic peak in the range between 55 °C and 120 °C with a peak at 87 °C. The curing conditions consisting of 24 h at 110 °C, followed by hot press post-curing at 180 °C, under 250 kN for one hour led to a cured thermoset with a glass transition temperature of 44 °C.

3.6 Interface strength between the epoxy thermoset matrix and reinforcing virgin fiber mesh

The interface region between the polymer and the fibers has distinct physicochemical properties and it is responsible for controlling the chemical, physical or interlocking interactions and therefore, it is a key contributor to the overall performance of fiber reinforced polymer composites.[55] Peeling adhesion tests and lap-shear bonding tests were performed in order to characterize the interface region between the TVx matrix and virgin v-UA, v-PDA and v-PDA-Si aramid meshes (the sample preparation and testing methodology are fully described in the ESI†). The outcomes from both tests suggested that the epoxy functionalized fibers (v-PDA-Si) led to an improved interface strength with the epoxy thermoset matrix, which was demonstrated by an increase in

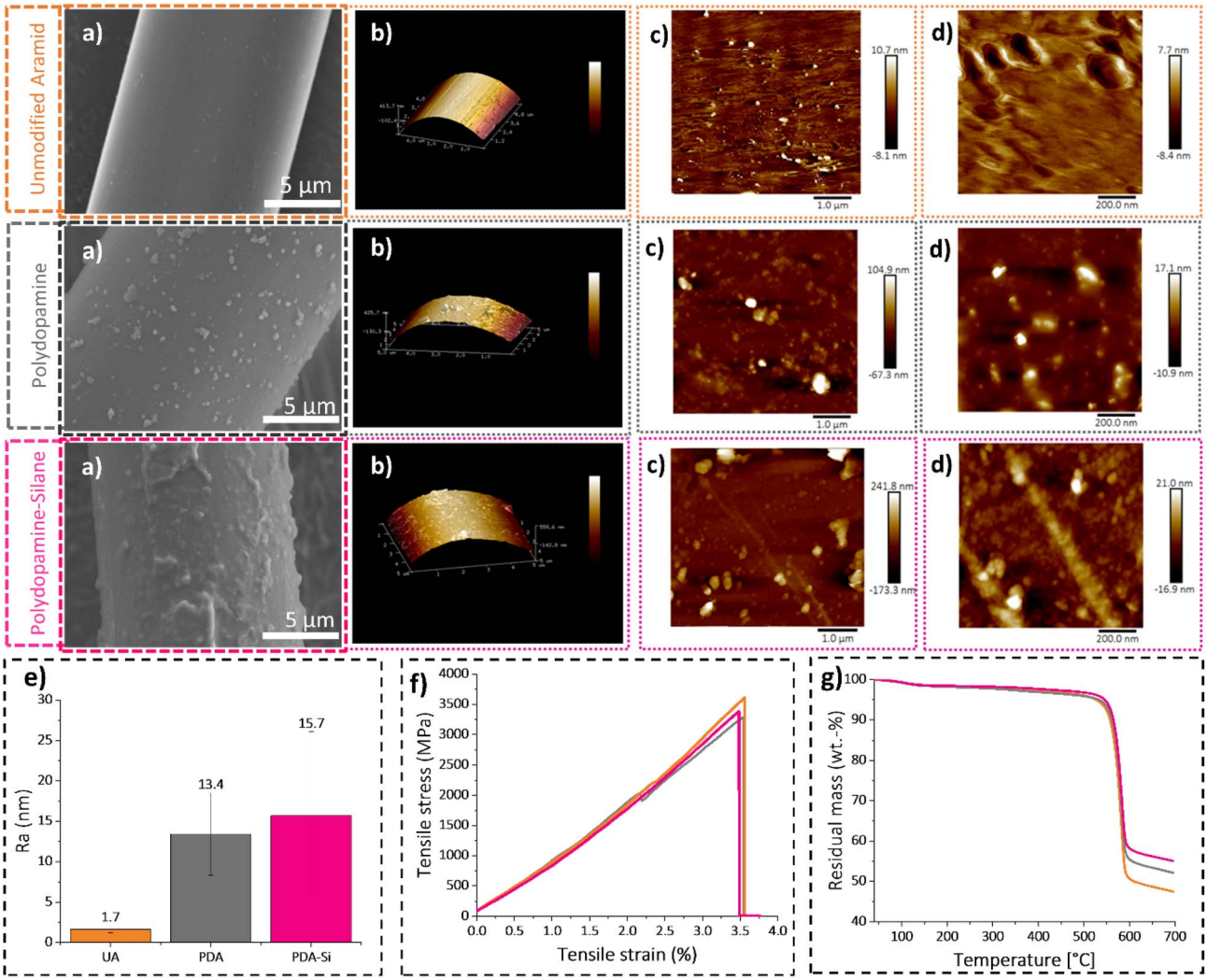

Fig. 4 (a) SEM images of the fiber surface, (b) AFM 3D view of the fiber surface with a scan size of 5 µm × 5 µm, (c) 2D view of the fiber topography with a scan size of 5 µm × 5 µm, (d) 2D view of the fiber topography with a scan size of 1 µm × 1 µm, and (e) calculated roughness parameters. (f) Mechanical properties and (g) thermogravimetric analysis of UA (orange), PDA (grey) and PDA Si (pink).

the peeling adhesion strength and maximum shear stress depicted in Fig. 5a and b. The values of peeling adhesion strength followed the trend: PDA-Si (457 ± 59 N m^{-1}) > UA (383 ± 60 N m^{-1}) > PDA (258 ± 34 N m^{-1}), which agrees with the lap-shear trends: PDA-Si (14.6 ± 1.8 MPa) > UA (10 ± 0.6 MPa) > PDA (8.4 ± 0.3 MPa). This is in line with the outcomes from previous studies reporting higher interfacial strength, shear strength and flexural strength values in the presence of silane coupling agents.[56,57] The mechanism behind this improvement is still under debate; however, contributions from chain entangling and covalent bonding appear to play an important role.[58] It was however unexpected that the obtained values for our PDA modified specimens were lower than the values recorded for UA meshes. This could be attributed to the formation of PDA agglomerates not strongly attached to the surface of the fibers, thereby weakening the interactions between the polymer and the surface of the fiber mesh. This is supported by the XPS (Table 1 and Fig. S4c†) and AFM results, which suggest that the incorporation of salts from the buffer solution and the formation of particle agglomerates might have taken place, thereby contributing to the formation of a weak boundary layer. Similar observations were previously reported,[57] as the bonding strength between an epoxy matrix and an aluminum surface coated with polydopamine presented lower adhesion strength than the untreated reference substrate, while an enhancement in the interface strength after a second functionalization step with an amino silane coupling agent was observed.

The SEM images of the aramid meshes after the peeling test further indicated distinct interactions resulting from the fiber functionalization (Fig. 5 c). UA meshes displayed small amounts of polymer on the surface and fiber fibrillation, which suggests that only physical interactions such as mechanical interlocking took place. PDA aramid meshes exhibited a clean detachment from the epoxy thermoset and therefore, remnants from the epoxy thermoset or indications

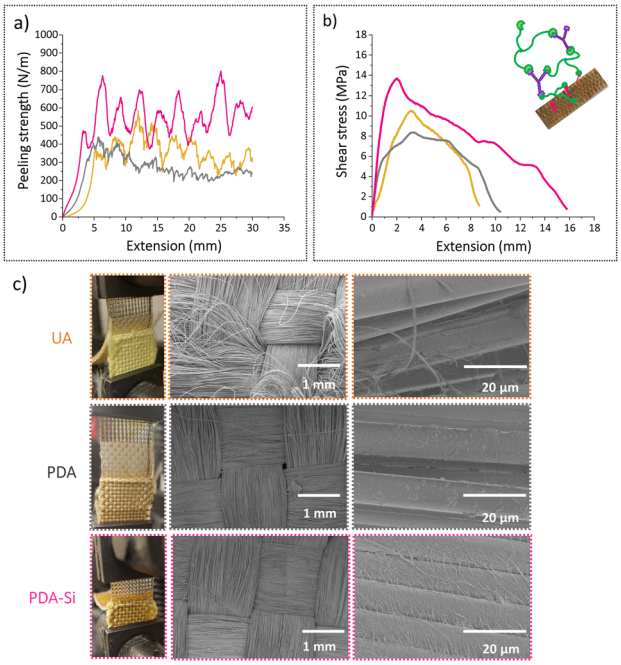

Fig. 5 Typical curves of (a) peeling adhesion tests and (b) lap shear tests. (c) SEM images of the meshes after peeling adhesion tests.

from mechanical interactions were not observed. As opposed to that, PDA-Si modified meshes remained covered with pieces of the thermoset material of different dimensions and polymer fibrils were observed over the analyzed surface, which suggests that the interactions in the interphase are stronger due to the potential formation of chemical bonds.

3.7 Composite preparation

Aramid composites were obtained by reinforcing the thermoset TVx with two layers of virgin UA, PDA or PDA-Si functionalized aramid meshes, which led to the bilayered composites shown in Fig. 6b. The spectroscopic characterization of the cured composites depicts the presence of the characteristic bands of the cured thermoset as previously described (Fig. 6b).

The thermogravimetric analysis (TGA) of the cured thermoset alone, Fig. S8,† showed a decomposition pathway in one step with a peak at 368 °C and an onset of decomposition, $T_{5\%}$ and $T_{10\%}$ at 268 °C and 312 °C respectively, suggesting that a thermally stable thermoset was obtained. The presence of the meshes led to a further increase in the thermal stability of the composites as suggested by the onset of decomposition $T_{5\%}$ at 285 °C and $T_{10\%}$ at 330 °C. It is worth noticing that a shift in the main decomposition step was also observed and it was more pronounced in the composites reinforced with PDA (374.7 ± 2.8 °C) and PDA-Si (375 ± 0.1 °C) compared to composites with UA (370.5 ± 0.2 °C), which suggests that the higher thermal stability of the functionalized fibers has a positive influence on the overall thermal resistance of the composites. Additionally, the second decomposition step observed in the thermogram at 580 °C, which corresponds to the degradation of aramid, was used to calculate the fiber loading in the composites and resulted in an average of 47 ± 6 wt%.

3.8 Chemical recycling of the virgin thermoset (TVx)

The high content of labile ester bonds, which are present in the virgin thermoset (TVx), enabled the evaluation of different chemical recycling methods, namely hydrolysis under acidic and basic conditions and mild solvolysis through transesterification exchange reactions. Thermoset hydrolysis under acidic (HCl 1 M) and basic conditions (NaOH 1 M) were initially evaluated; however, acidic hydrolysis proved to be an ineffective method, and basic hydrolysis was detrimental for the surface functionalization (for details see the ESI†).

In view of this, a mild solvolysis through transesterification exchange reactions was pursued. The use of ethylene glycol as a solvent and zinc acetate as the transesterification catalyst resulted in a homogeneous and translucid solution (Fig. 7a). The evaporation of residual solvent generated a viscous resin consisting of a mixture of oligomers with a number average and weight average molecular weight of 716 g mol^{-1} and 2291 g mol^{-1}, respectively (Fig. S12†). Spectroscopic characterization by ^{1}H and ^{13}C NMR suggests the formation of oligomeric structures rich in hydroxyl and ester groups resulted from the transesterification exchange reactions with ethylene glycol, in Fig. 7b and S13.†

The curing reaction of the obtained viscous resin was followed by DSC, where an exotherm at 97 °C corresponding to the curing reaction was determined (Fig. S12†). The curing reaction by hot pressing at 180 °C for 1 h and 250 kN resulted in a flexible recycled thermoset (TRx). However, the mechanical properties

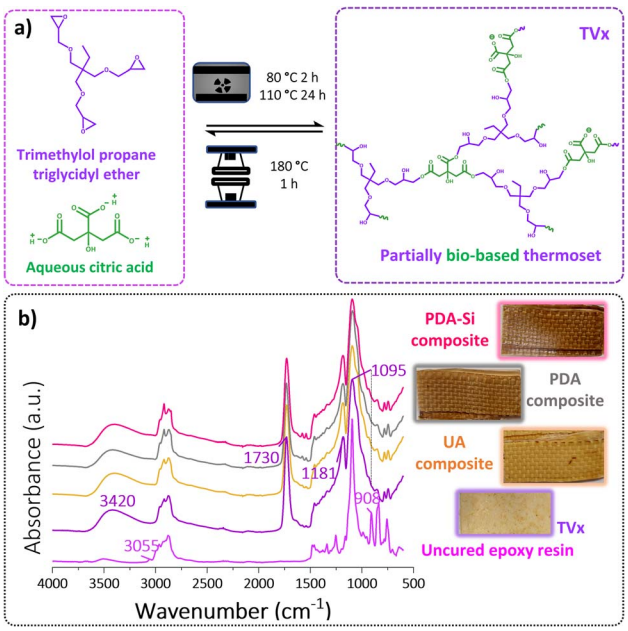

Fig. 6 (a) Chemical structure of the uncured epoxy resin and citric acid and the proposed structure of the cured thermoset. (b) Acquired ATR-FTIR spectra of the aforementioned samples and physical appearance of the TVx and UA, PDA and PDA-Si composites.

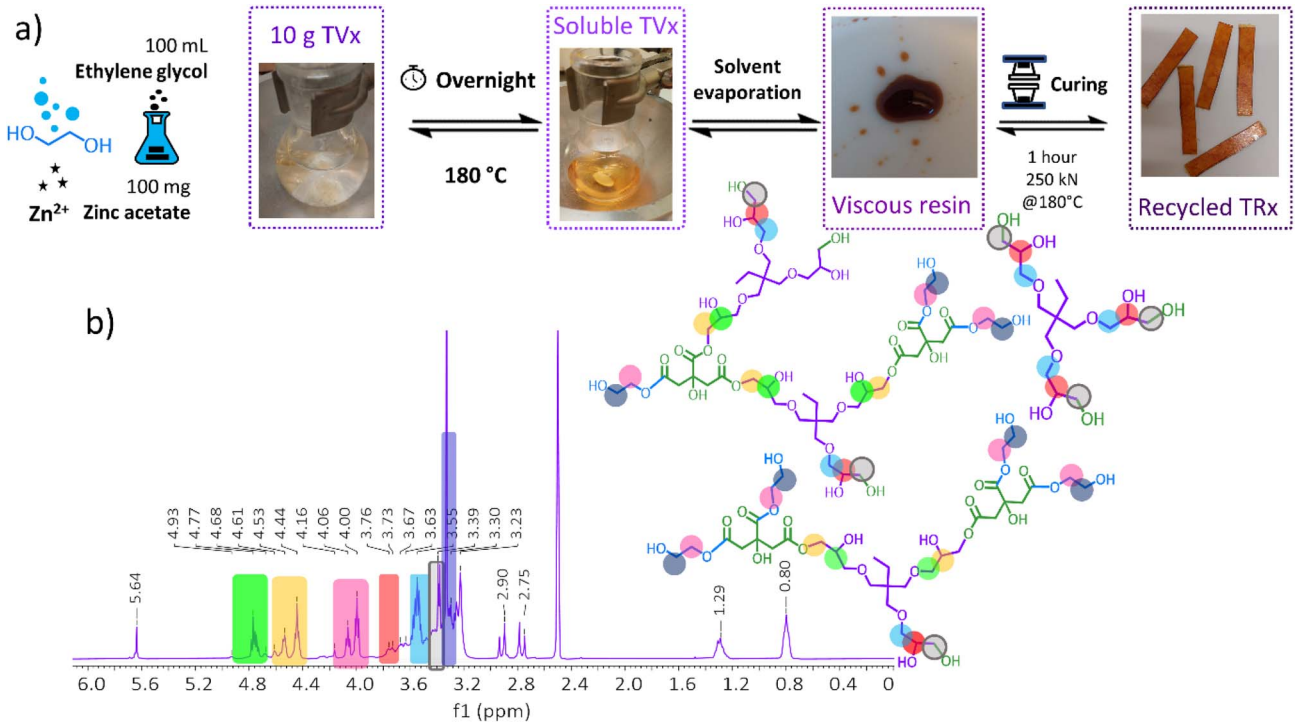

Fig. 7 (a) Chemical recycling methodology through transesterification exchange reactions. (b) Spectroscopic characterization of the viscous resin performed in deuterated DMSO by ^{1}H NMR.

of TRx presented an abrupt loss, which was unavoidable even upon a 50/50 wt% mixture of recovered resin and virgin material. This was manifested by a 33% recovery of the tensile stress at break and 83% recovery of the tensile strain in comparison with the virgin thermoset (Fig. S14†).

FTIR of the cured TRx (Fig. S15a†) suggests the formation of an ester-based thermoset with an increased abundance of primary hydroxyl groups. The bands at 1274 cm^{-1} and 1038 cm^{-1} correspond to C–OH in plane deformations and C–O stretching vibrations. The high concentration of free hydroxyls can increase the free volume and lower the crosslinking density within TRx.[33] Additionally, these active groups can lead to etherification reactions, which would act as flexible segments resulting in an increased chain mobility. With that in mind, the chemical structure of the recycled TRx which is proposed in Fig. S15b† would explain the observed decrease in the mechanical properties and lower crosslinking density, which is supported by the decrease in Tg depicted in Fig. S15c.†

In view of the high content of hydroxyl groups in the TRx matrix, we hypothesized that the adhesion strength with the

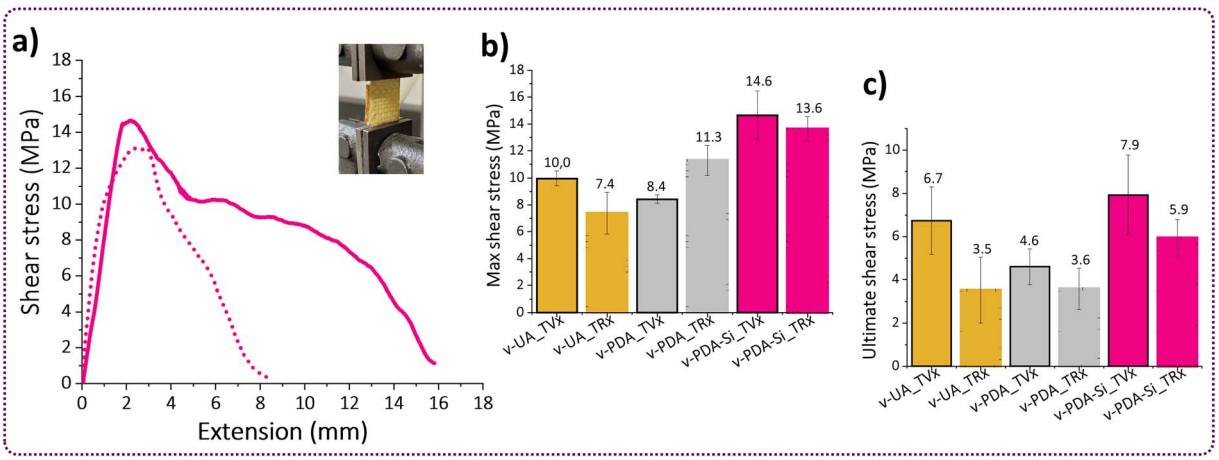

Fig. 8 (a) Characteristic lap-shear curves of v-PDA-Si specimens with TVx (solid line) and TRx (dotted line). Comparison of the (b) maximum shear stress and (c) ultimate shear stress in the lap-shear test with v-UA, v-PDA and v-PDA Si meshes with virgin and recycled thermosets (TVx and TRx).

aramid meshes would not deteriorate. The reason is that the high availability of hydroxyl groups can increase the bonding strength with different substrates having the potential to establish hydrogen bonding or covalent interactions and this is precisely the chemistry that has been exploited for the development of highly adhesive materials.[59–61] We evaluated the adhesion strength between the TRx and virgin aramid meshes v-UA, v-PDA and v PDA-Si by lap shear tests and compared it to the adhesion strength obtained with virgin TVx. Our results suggest that the bonding characteristics of TRx promoted good adhesion with v-PDA-Si aramid meshes and lead to a recovery of 93% and 75% of the maximum and ultimate shear stress, respectively. The reduction of ultimate shear stress and total extension may suggest that secondary interactions such as hydrogen bonding enabled a good retention of the maximum shear at low extensions. However, these secondary interactions are not strong enough to bear the load upon further extension (Fig. 8d). These are the typical characteristics of ductile adhesive.[60] On the other hand, a comparison with the bonding characteristics of v-UA and v-PDA corroborated that v-PDA-Si had the highest interfacial interactions among the three tested meshes (Fig. 8e). Additionally, it was observed that even when v-UA exhibited a maximum shear recovery of 74%, it was below the maximum shear obtained for the v-PDA meshes. This is in contrast to the peeling adhesion and the outcome with virgin TVx. This can be attributed to the high content of amines and hydroxyl groups in the catecholamine structure of PDA, that have the potential to establish a large number of hydrogen bonds, and the increased chain mobility in TRx, which can improve fiber wetting and further benefit the mechanical interlocking mechanisms.[57] Additionally, the increased fluid-like behavior of TRx can facilitate access to the underlying fiber layers of the mesh resulting in an interaction, not only on the surface, but also within the inner layers of the mesh.

3.9 Chemical recycling of aramid reinforced composites

The composites prepared with virgin TVx reinforced with two layers of v-UA, v-PDA or v-PDA Si meshes were chemically recycled through transesterification exchange reactions. This methodology resulted in the recovery of the two layers of r-UA, r-

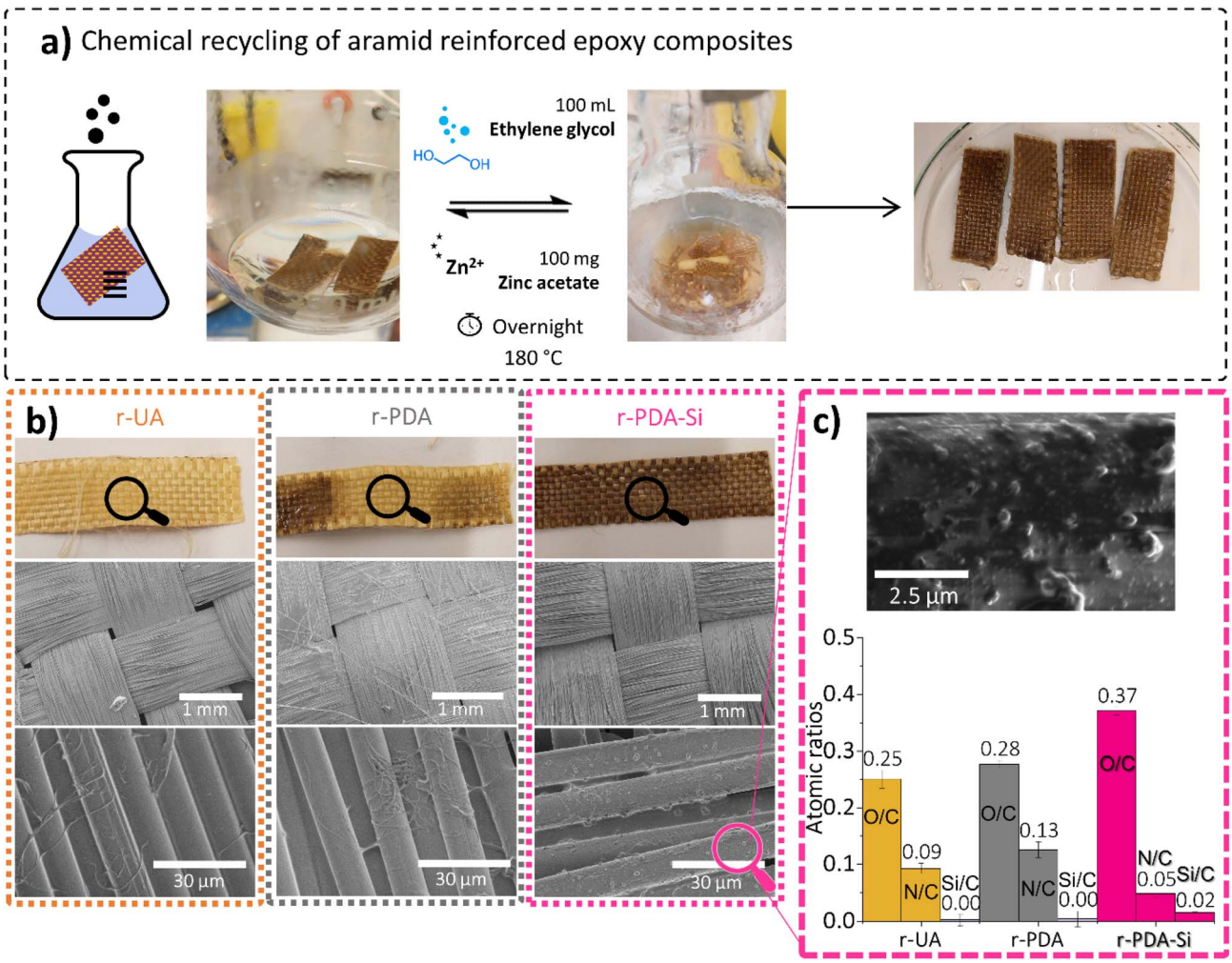

Fig. 9 (a) Chemical recycling of aramid reinforced epoxy composites through transesterification exchange reactions. (b) Recovered r-UA, r-PDA and r-PDA-Si meshes after chemical recycling and SEM characterization. (c) SEM image of a PDA-Si fiber depicting the retention of the surface functionality supported by atomic ratios determined from the EDS measurements.

PDA and r-PDA-Si meshes, which appeared free of polymer on plain sight. An evident removal of TVx from the surface of r-UA, r-PDA and r-PDA-Si aramid meshes was seen by SEM. The scarce remnants from the matrix consisted of small polymer fibrils. The chemical recycling procedure leads to clear differences between the recovered r-PDA and r-PDA-Si meshes (Fig. 9b). On one hand, r-PDA meshes presented a clear discoloration on the surface of the mesh, which can indicate that the polydopamine coating was affected by the chemical recycling method. The smooth fiber topography observed by SEM further suggested the loss of the rough PDA coating. This was confirmed by the FTIR spectroscopic characterization in Fig. S17,† where the bands associated with PDA are no longer present. In contrast, recycled r-PDA-Si meshes retained the original dark brown color and the morphology of the functionalization, as suggested by SEM images (Fig. 9c). The spectroscopic characterization in Fig. 10a further suggests the existence of the coating, which was indicated by the presence of bands around 1613 cm^{-1}, 1484 cm^{-1} and 1250 cm^{-1}, which were previously associated with the expected chemistry of the surface functionality. This was supported by EDS, which revealed that r-PDA-Si had higher O/C and Si/C ratios and a lower N/C ratio in comparison with r-UA and r-PDA (Fig. 9c). This suggests that the silane functionalization was retained after the chemical recycling method.

The outcome agrees with the results obtained after the Soxhlet extraction with ethanol. The analysis of the extracted fibers revealed that the rough features of polydopamine on PDA coated fibers were significantly reduced (Fig. S18a†). In contrast, PDA-Si functionalized fibers maintained the characteristic features from the functionalization (Fig. S18b†). This was spectroscopically ascertained by SEM-EDS, where Si was still detected with a concentration of 5.1 ± 1.6 wt% (Table S6†).

The striking difference observed between r-PDA and r-PDA-Si can be explained by the distinct chemistry involved in each of the functionalization steps. As stated in previous studies, the self-adhesion of polydopamine on a wide variety of substrates is thought to be reliant on secondary interactions such as hydrogen bonding and π–π interactions.[17,43,45,62] Conversely, the condensation reaction of the silane coupling agent involves the formation of more robust O–Si–C covalent bonds[56] giving rise to a functionalized layer of higher stability.

Additional characterization of the recovered r-PDA-Si meshes suggests that 82% of the TVx matrix was successfully removed from the aramid meshes as clearly shown in the TGA analysis (Fig. 10b). As opposed to the two-step decomposition of the composite, corresponding to the thermoset and the fiber mesh, the main decomposition step of r-PDA-Si takes place at 584 °C, which corresponds to the thermal degradation of aramid meshes. The spectroscopic analysis in Fig. 10a revealed that the surface of the r-PDA-Si meshes was practically clean from the bands associated with the TVx resin. This result seems to imply that the residues from the TVx matrix detected by TGA (18%) were present within the inner fiber layers within the mesh. Higher mixing rates could have proved beneficial in order to reach the residual matrix in the inner layers of the mesh. However, this would unavoidably result in the loss of the weaving form and shape. This would cause the downgrading of

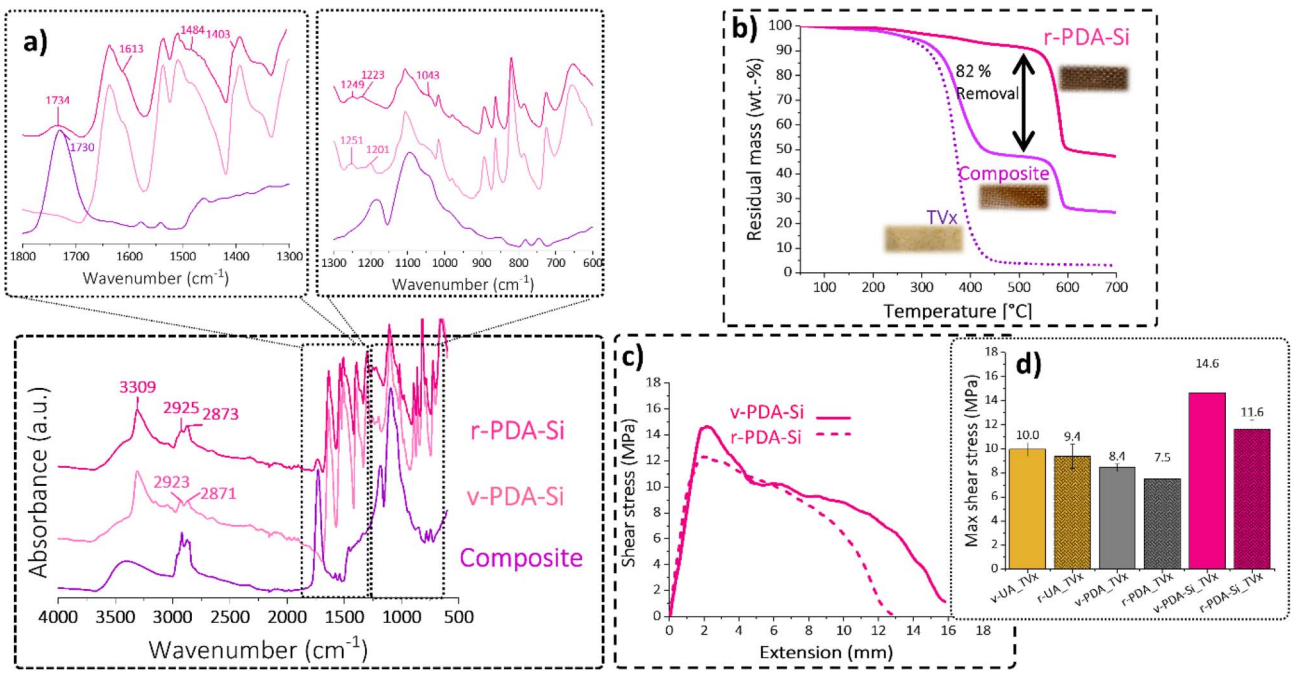

Fig. 10 (a) Spectroscopic characterization of recovered r-PDA-Si depicting the removal of the thermoset matrix supported by (b) thermogravimetric analysis indicating a removal of 82% of the thermoset matrix. (c) Typical lap-shear test curves comparing the performance of v-PDA-Si and r-PDA-Si after chemical recycling. (d) Comparison of the maximum shear stress obtained with UA, PDA and PDA-Si meshes in their virgin state and after chemical recycling.

the recycled mesh implying a decrease in the sustainability of the proposed methodology. In fact, it is precisely this feature which keeps hindering the application of chemical recycling methods on a larger scale and up to now, a considerable amount of the existing research has shown that a complete removal of the polymer matrix from carbon fiber meshes has been reached at a stake of the weaving features. An interesting example showed that in order to retain the weaving geometry of a carbon fiber mesh, only a partial removal of 90% of the resin was attainable.[40]

Despite the current limitation, it has been commonly assumed that the surface of the meshes plays the most important role when it comes to establishing good interactions with the polymer matrix. Our results from the previous discussion suggest that the surface of the recovered r-PDA-Si meshes is not only adequately free from TVx residues but still bears the surface functionality required to achieve good interfacial interactions. This hypothesis was tested by lap shear analysis with specimens composed of recovered r-UA, r-PDA and r-PDA-Si meshes and the virgin TVx matrix. The results from this analysis corroborate that r-PDA-Si retained 79% of the maximum shear and 91% of the ultimate shear (Fig. 10c). It was further observed that the imposed load could still be maintained up to 76% of the total extension in comparison to virgin v-PDA-Si. It is worth noticing that the recycled r-PDA-Si reached a bonding strength comparable to that of virgin v-UA and v-PDA.

4 Conclusions

Aramid meshes were successfully functionalized through a mild modification process, which improved the performance and chemical recyclability of epoxy/aramid mesh composites. Specifically, the functionalization with polydopamine and a silane coupling agent (PDA-Si) enhanced the interfacial strength between v-PDA-Si meshes and virgin TVx as demonstrated by a 46% increase in the lap shear stress values when compared to the unmodified reference. This surface functionalization was highly beneficial in the chemical recycling process and enabled the recovery of high-quality fiber meshes with a high retention of the fiber functionality. This was ascertained by thermogravimetric, spectroscopic and microscopic characterization of the recovered PDA-Si meshes and also by lap shear tests showing 73% retention of lap shear stress. The value of transesterification exchange reactions as a way to impart chemical recyclability to epoxy thermosets reinforced with aramid fiber meshes was illustrated, proving that its application in fiber reinforced polymer composites is not only restricted to composites reinforced with carbon and glass fibers, but can also be applied to more sensitive fibers such as aramid. In all, the results demonstrate that, besides the well documented performance enhancement, fiber surface functionalization can play a key role in the development of future recycling strategies for FRPCs by enabling the recovery of high-quality surface functionalized fibers. Such fibers can be reused in similar applications without a significant downgrading.

Conflicts of interest

There are no conflicts to declare.

Acknowledgements

This research forms part of the research program of Dutch Polymer Institute, DPI, Project #843; Recyclable high-performance composites with reversible bonding.

Notes and references

1 A. Bardow, M. Bachmann, C. Zibunas, J. Hartmann and G. Guillén-gosálbez, Towards Circular Plastics within Planetary Boundaries, *Nat. Sustain.*, 2022, 1–23, DOI: 10.1038/s41893-022-01054-9.

2 G. Lin, H. Wang, B. Yu, G. Qu, S. Chen, T. Kuang, K. Yu and Z. Liang, Combined Treatments of Fiber Surface Etching/Silane-Coupling for Enhanced Mechanical Strength of Aramid Fiber-Reinforced Rubber Blends, *Mater. Chem. Phys.*, 2020, **255**, 123486, DOI: 10.1016/j.matchemphys.2020.123486.

3 J. Zhao, Effect of Surface Treatment on the Structure and Properties of Para-Aramid Fibers by Phosphoric Acid, *Fibers Polym.*, 2013, **14**(1), 59–64, DOI: 10.1007/s12221-013-0059-x.

4 P. J. De Lange and P. G. Akker, Adhesion Activation of Twaron Aramid Fibers for Application in Rubber: Plasma Versus Chemical Treatment, *J. Adhes. Sci. Technol.*, 2012, **26**(6), 827–839, DOI: 10.1163/016942411X580036.

5 P. J. De Lange, P. G. Akker, S. Willemsen and R. N. Datta, The Effect of Oily Finish Components on the Adhesion between Aramid Fibers and Rubber, *J. Adhes. Sci. Technol.*, 2009, **23**(1), 139–149, DOI: 10.1163/156856108X344568.

6 M. Xi, Y. L. Li, S. yong Shang, D. H. Li, Y. X. Yin and X. Y. Dai, Surface Modification of Aramid Fiber by Air DBD Plasma at Atmospheric Pressure with Continuous On-Line Processing, *Surf. Coat. Technol.*, 2008, **202**(24), 6029–6033, DOI: 10.1016/j.surfcoat.2008.06.181.

7 C. X. Wang, M. Du, J. C. Lv, Q. Q. Zhou, Y. Ren, G. L. Liu, D. W. Gao and L. M. Jin, Surface Modification of Aramid Fiber by Plasma Induced Vapor Phase Graft Polymerization of Acrylic Acid. I. Influence of Plasma Conditions, *Appl. Surf. Sci.*, 2015, **349**, 333–342, DOI: 10.1016/j.apsusc.2015.05.036.

8 S. R. Wu, G. S. Sheu and S. S. Shyu, Kevlar Fiber-Epoxy Adhesion and Its Effect on Composite Mechanical and Fracture Properties by Plasma and Chemical Treatment, *J. Appl. Polym. Sci.*, 1996, **62**(9), 1347–1360, DOI: 10.1002/(SICI)1097-4628(19961128)62:9<1347::AID-APP5>3.0.CO;2-H.

9 P. J. De Lange, P. G. Akker, A. J. H. Maas, A. Knoester and H. H. Brongersma, Adhesion Activation of Twaron ® Aramid Fibres Studied with Low-Energy Ion Scattering and x-Ray Photoelectron Spectroscopy, *Surf. Interface Anal.*, 2001, **31**(12), 1079–1084, DOI: 10.1002/sia.1147.

10 H. J. Kim and J. H. Song, Improvement in the Mechanical Properties of Carbon and Aramid Composites by Fiber

Surface Modification Using Polydopamine, *Composites, Part B*, 2019, **160**, 31–36, DOI: 10.1016/j.compositesb.2018.10.027.

11 S. Chen, Y. Cao and J. Feng, Polydopamine as an Efficient and Robust Platform to Functionalize Carbon Fiber for High-Performance Polymer Composites, *ACS Appl. Mater. Interfaces*, 2014, **6**(1), 349–356, DOI: 10.1021/am404394g.

12 S. D. Mun, S.-J. Lee and J. H. Song, Tensile Properties and Surface Treatment of Fiber Composites with the Concentration of Polydopamine and Buffer Solution, *Fibers Polym.*, 2021, **22**(1), 249–255, DOI: 10.1007/s12221-021-1162-z.

13 X. Yang, Q. Tu, X. Shen, Q. Yin, M. Pan, C. Jiang and C. Hu, Enhancing the Interfacial Adhesion with Rubber Matrix by Grafting Polydopamine-Carbon Nanotubes onto Poly(p-Phenylene Terephthalamide) Fibers, *Polymers*, 2019, **11**(8), 1231, DOI: 10.3390/polym11081231.

14 K. Cheng, M. Li, S. Zhang, M. He, J. Yu, Y. Feng and S. Lu, Study on the Structure and Properties of Functionalized Fibers with Dopamine, *Colloids Surf., A*, 2019, **582**, 123846, DOI: 10.1016/j.colsurfa.2019.123846.

15 W. Gu, X. Liu, Q. Ye, Q. Gao, S. Gong, J. Li and S. Q. Shi, Bio-Inspired Co-Deposition Strategy of Aramid Fibers to Improve Performance of Soy Protein Isolate-Based Adhesive, *Ind. Crops Prod.*, 2020, **150**, 112424, DOI: 10.1016/J.INDCROP.2020.112424.

16 R. Sa, Y. Yan, Z. Wei, L. Zhang, W. Wang and M. Tian, Surface Modification of Aramid Fibers by Bio-Inspired Poly(Dopamine) and Epoxy Functionalized Silane Grafting, *ACS Appl. Mater. Interfaces*, 2014, **6**(23), 21730–21738, DOI: 10.1021/am507087p.

17 H. Lee, S. M. Dellatore, W. M. Miller and P. B. Messersmith, Mussel-Inspired Surface Chemistry for Multifunctional Coatings, *Science*, 2007, **318**(5849), 426–430, DOI: 10.1126/science.1147241.

18 J. Yuan, Z. Zhang, M. Yang, F. Guo, X. Men and W. Liu, Surface Modification of Hybrid-Fabric Composites with Amino Silane and Polydopamine for Enhanced Mechanical and Tribological Behaviors, *Tribol. Int.*, 2017, **107**, 10–17, DOI: 10.1016/J.TRIBOINT.2016.11.013.

19 T. Xu, J. Tian, L. An, Y. Jiao, Q. Yin and Y. Tan, Study on the Construction of Dopamine/Poly(Ethyleneimine)/Aminoated Carbon Nanotube Multilayer Films on Aramid Fiber Surfaces to Improve the Mechanical Properties of Aramid Fibers/Epoxy Composites, *ACS Omega*, 2022, **7**(40), 35610–35625, DOI: 10.1021/ACSOMEGA.2C03390/ASSET/IMAGES/LARGE/AO2C03390_0017.JPEG.

20 L. Zeng, X. Liu, X. Chen and C. Soutis, Surface Modification of Aramid Fibres with Graphene Oxide for Interface Improvement in Composites, *Appl. Compos. Mater.*, 2018, **25**(4), 843–852, DOI: 10.1007/S10443-018-9718-9/FIGURES/7.

21 X. Gong, Y. Liu, Y. Wang, Z. Xie, Q. Dong, M. Dong, H. Liu, Q. Shao, N. Lu, V. Murugadoss, T. Ding and Z. Guo, Amino Graphene Oxide/Dopamine Modified Aramid Fibers: Preparation, Epoxy Nanocomposites and Property Analysis, *Polymer*, 2019, **168**, 131–137, DOI: 10.1016/J.POLYMER.2019.02.021.

22 J. Tian, L. An, Y. Tan, T. Xu, X. Li and G. Chen, Graphene Oxide-Modified Aramid Fibers for Reinforcing Epoxy Resin Matrixes, *ACS Appl. Nano Mater.*, 2021, **4**(9), 9595–9605, DOI: 10.1021/ACSANM.1C02017/SUPPL_FILE/AN1C02017_SI_001.PDF.

23 K. Yu, Q. Shi, M. L. Dunn, T. Wang and H. J. Qi, Carbon Fiber Reinforced Thermoset Composite with Near 100% Recyclability, *Adv. Funct. Mater.*, 2016, **26**(33), 6098–6106, DOI: 10.1002/adfm.201602056.

24 H. Si, L. Zhou, Y. Wu, L. Song, M. Kang, X. Zhao and M. Chen, Rapidly Reprocessable, Degradable Epoxy Vitrimer and Recyclable Carbon Fiber Reinforced Thermoset Composites Relied on High Contents of Exchangeable Aromatic Disulfide Crosslinks, *Composites, Part B*, 2020, **199**, 108278, DOI: 10.1016/j.compositesb.2020.108278.

25 T. Liu, L. Shao, B. Zhao, Y. C. Chang and J. Zhang, Progress in Chemical Recycling of Carbon Fiber Reinforced Epoxy Composites, *Macromol. Rapid Commun.*, 2022, **2200538**, 1–21, DOI: 10.1002/marc.202200538.

26 S. Kumar and S. Krishnan, Recycling of Carbon Fiber with Epoxy Composites by Chemical Recycling for Future Perspective: A Review, *Chem. Pap.*, 2020, **74**(11), 3785–3807, DOI: 10.1007/s11696-020-01198-y.

27 M. Shen and M. L. Robertson, Degradation Behavior of Biobased Epoxy Resins in Mild Acidic Media, *ACS Sustainable Chem. Eng.*, 2021, **9**, 438–447, DOI: 10.1021/acssuschemeng.0c07621.

28 C. Di Mauro, T. N. Tran, A. Graillot and A. Mija, Enhancing the Recyclability of a Vegetable Oil-Based Epoxy Thermoset through Initiator Influence, *ACS Sustain. Chem. Eng.*, 2020, **8**(20), 7690–7700, DOI: 10.1021/acssuschemeng.0c01419.

29 I. Vollmer, M. J. F. Jenks, M. C. P. Roelands, R. J. White, T. van Harmelen, P. de Wild, G. P. van der Laan, F. Meirer, J. T. F. Keurentjes and B. M. Weckhuysen, Beyond Mechanical Recycling: Giving New Life to Plastic Waste, *Angew. Chem., Int. Ed.*, 2020, **59**(36), 15402–15423, DOI: 10.1002/anie.201915651.

30 L. Zhong, Y. Hao, J. Zhang, F. Wei, T. Li, M. Miao and D. Zhang, Closed-Loop Recyclable Fully Bio-Based Epoxy Vitrimers from Ferulic Acid-Derived Hyperbranched Epoxy Resin, *Macromolecules*, 2022, **55**(2), 595–607, DOI: 10.1021/acs.macromol.1c02247.

31 Y. Liu, Z. Yu, B. Wang, P. Li, J. Zhu and S. Ma, Closed-Loop Chemical Recycling of Thermosetting Polymers and Their Applications: A Review, *Green Chem.*, 2022, **24**(15), 5691–5708, DOI: 10.1039/d2gc00368f.

32 W. Zhang, J. Wu, L. Gao, B. Zhang, J. Jiang and J. Hu, Recyclable, Reprocessable, Self-Adhered and Repairable Carbon Fiber Reinforced Polymers Using Full Biobased Matrices from Camphoric Acid and Epoxidized Soybean Oil, *Green Chem.*, 2021, **23**(7), 2763–2772, DOI: 10.1039/d1gc00648g.

33 Q. Mu, L. An, Z. Hu and X. Kuang, Fast and Sustainable Recycling of Epoxy and Composites Using Mixed Solvents, *Polym. Degrad. Stab.*, 2022, **199**, 109895, DOI: 10.1016/j.polymdegradstab.2022.109895.

34 T. Maeda, H. Otsuka and A. Takahara, Dynamic Covalent Polymers: Reorganizable Polymers with Dynamic Covalent Bonds, *Prog. Polym. Sci.*, 2009, 581–604, DOI: 10.1016/j.progpolymsci.2009.03.001.

35 X. Kuang, Y. Zhou, Q. Shi, T. Wang and H. J. Qi, Recycling of Epoxy Thermoset and Composites via Good Solvent Assisted and Small Molecules Participated Exchange Reactions, *ACS Sustain. Chem. Eng.*, 2018, **6**(7), 9189–9197, DOI: 10.1021/acssuschemeng.8b01538.

36 E. Schamel, G. Wehnert, H. Schlachter and D. Söthje, Chemical Recycling of Carbon Fiber Reinforced Epoxy Composites Using Mild Conditions, *Chem.-Ing.-Tech.*, 2021, **93**(10), 1619–1628, DOI: 10.1002/cite.202100048.

37 Y. Y. Liu, G. L. Liu, Y. D. Li, Y. Weng and J. B. Zeng, Biobased High-Performance Epoxy Vitrimer with UV Shielding for Recyclable Carbon Fiber Reinforced Composites, *ACS Sustain. Chem. Eng.*, 2021, **9**(12), 4638–4647, DOI: 10.1021/acssuschemeng.1c00231.

38 M. Lejeail and H. R. Fischer, Development of a Completely Recyclable Glass Fiber-Reinforced Epoxy Thermoset Composite, *J. Appl. Polym. Sci.*, 2021, **138**(3), 1–15, DOI: 10.1002/app.49690.

39 D. Zhou, H. Huang, Y. Wang, J. Yu and Z. Hu, Design and Synthesis of an Amide-Containing Crosslinked Network Based on Diels-Alder Chemistry for Fully Recyclable Aramid Fabric Reinforced Composites, *Compos. Sci. Technol.*, 2020, **197**, 108280, DOI: 10.1016/j.compscitech.2020.108280.

40 W. Ballout, N. Sallem-Idrissi, M. Sclavons, C. Doneux, C. Bailly, T. Pardoen and P. Van Velthem, High Performance Recycled CFRP Composites Based on Reused Carbon Fabrics through Sustainable Mild Solvolysis Route, *Sci. Rep.*, 2022, **12**(1), 1–15, DOI: 10.1038/s41598-022-09932-0.

41 W. Post, A. Susa, R. Blaauw, K. Molenveld and R. J. I. Knoop, A Review on the Potential and Limitations of Recyclable Thermosets for Structural Applications, *Polym. Rev.*, 2020, **60**(2), 359–388, DOI: 10.1080/15583724.2019.1673406.

42 Y. Yang, Y. Xu, Y. Ji and Y. Wei, Functional Epoxy Vitrimers and Composites, *Prog. Mater. Sci.*, 2020, 100710, DOI: 10.1016/j.pmatsci.2020.100710.

43 J. Liebscher, H. A. Scheidt, C. Filip, R. Turcu, A. Bende and S. Beck, Structure of Polydopamine: A Never-Ending Story?, *Langmuir*, 2013, **29**, 10539–10548, DOI: 10.1021/la4020288.

44 R. A. Zangmeister, T. A. Morris and M. J. Tarlov, Characterization of Polydopamine Thin Films Deposited at Short Times by Autoxidation of Dopamine, *Langmuir*, 2013, **29**(27), 8619–8628, DOI: 10.1021/LA400587J.

45 J. H. Ryu, P. B. Messersmith and H. Lee, Polydopamine Surface Chemistry: A Decade of Discovery, *ACS Appl. Mater. Interfaces*, 2018, 7523–7540, DOI: 10.1021/acsami.7b19865.

46 P. J. De Lange and P. G. Akker, Adhesion Activation of Twaron Aramid Fibers for Application in Rubber: Plasma Versus Chemical Treatment, *J. Adhes. Sci. Technol.*, 2012, **26**(6), 827–839, DOI: 10.1163/016942411X580036.

47 K. Shimizu, H. Habazaki, P. Skeldon and G. E. Thompson, Adhesion Activation of Twaron® Aramid Fibres Studied with Low-Energy Ion Scattering and x-Ray Photoelectron Spectroscopy, *Surf. Interface Anal.*, 2001, **31**(12), 1079–1084, DOI: 10.1002/sia.1147.

48 M. G. Dobb and R. M. Robson, Structural Characteristics of Aramid Fibre Variants, *J. Mater. Sci.*, 1990, **25**(1), 459–464, DOI: 10.1007/BF00714056.

49 J. Liebscher, Chemistry of Polydopamine – Scope, Variation, and Limitation, *Eur. J. Org. Chem.*, 2019, **2019**(31–32), 4976–4994, DOI: 10.1002/ejoc.201900445.

50 F. I. Altuna, J. Antonacci, G. F. Arenas, V. Pettarin, C. E. Hoppe and R. J. J. Williams, Photothermal Triggering of Self-Healing Processes Applied to the Reparation of Bio-Based Polymer Networks, *Mater. Res. Express*, 2016, **3**(4), 045003, DOI: 10.1088/2053-1591/3/4/045003.

51 S. Mu, Y. Zhang, J. Zhou, B. Wang and Z. Wang, Recyclable and Mechanically Robust Palm Oil-Derived Epoxy Resins with Reconfigurable Shape-Memory Properties, *ACS Sustain. Chem. Eng.*, 2020, **8**(13), 5296–5304, DOI: 10.1021/acssuschemeng.0c00443.

52 F. I. Altuna, V. Pettarin and R. J. J. Williams, Self-Healable Polymer Networks Based on the Cross-Linking of Epoxidised Soybean Oil by an Aqueous Citric Acid Solution, *Green Chem.*, 2013, **15**(12), 3360–3366, DOI: 10.1039/c3gc41384e.

53 M. Pawar, A. Kadam, O. Yemul, V. Thamke and K. Kodam, Biodegradable Bioepoxy Resins Based on Epoxidized Natural Oil (Cottonseed & Algae) Cured with Citric and Tartaric Acids through Solution Polymerization: A Renewable Approach, *Ind. Crops Prod.*, 2016, **89**, 434–447, DOI: 10.1016/j.indcrop.2016.05.025.

54 G. Socrates, *Infrared Characteristic Group Frequencies*, John Wiley & Sons, Ltd., Chichester, England, 2001, DOI: 10.1016/0160-9327(81)90159-9.

55 J. Karger-Kocsis, H. Mahmood and A. Pegoretti, Recent Advances in Fiber/Matrix Interphase Engineering for Polymer Composites, *Prog. Mater. Sci.*, 2015, **73**, 1–43, DOI: 10.1016/J.PMATSCI.2015.02.003.

56 E. P. Plueddemmann, *Silane Coupling Agents*, Springer Science + Business Media New York, New York, 2nd edn, 1991, vol. 1, DOI: 10.1016/0143-7496(92)90011-j.

57 N. T. Tran, D. P. Flanagan, J. A. Orlicki, J. L. Lenhart, K. L. Proctor and D. B. Knorr, Polydopamine and Polydopamine-Silane Hybrid Surface Treatments in Structural Adhesive Applications, *Langmuir*, 2018, **34**(4), 1274–1286, DOI: 10.1021/acs.langmuir.7b03178.

58 L. W. Jenneskens, Adhesion Improvements by Silane Coupling Agents in Composites, in *Interfacial Phenomena in Composite Materials '91*, 1991, p. iii, DOI: 10.1016/b978-0-7506-0356-0.50001-0.

59 N. T. Tran, A. J. Boyer and D. B. Knorr, Multiple Local Hydroxyl Groups as a Way to Improve Bond Strength and Durability in Structural Adhesives, *J. Adhes.*, 2022, **98**(12), 1834–1854, DOI: 10.1080/00218464.2021.1939692.

60 M. A. Rahman, C. Bowland, S. Ge, S. R. Acharya, S. Kim, V. R. Cooper, X. Chelsea Chen, S. Irle, A. P. Sokolov, A. Savara and T. Saito, Design of Tough Adhesive from Commodity Thermoplastics through Dynamic

Crosslinking, *Sci. Adv.*, 2021, **7**(42), 1–12, DOI: **10.1126/sciadv.abk2451**.

61 A. Narayanan, S. Kaur, N. Kumar, M. Tsige, A. Joy and A. Dhinojwala, Cooperative Multivalent Weak and Strong Interfacial Interactions Enhance the Adhesion of Mussel-Inspired Adhesives, *Macromolecules*, 2021, **54**(12), 5417–5428, DOI: **10.1021/acs.macromol.1c00742**.

62 A. Postma, Y. Yan, Y. Wang, A. N. Zelikin, E. Tjipto and F. Caruso, Self-Polymerization of Dopamine as a Versatile and Robust Technique to Prepare Polymer Capsules, *Chem. Mater.*, 2009, **21**(14), 3042–3044, DOI: **10.1021/cm901293e**.